# XPS Analysis of Zeolitic Materials

H. Shimada, K. Sato, Y. Nishimura, N. Matsubayashi, M. Imamura
*National Institute of Materials and Chemical Research, Tsukuba, Ibaraki 305-8565 Japan*

(Received October 30 1998; accepted January 13 1999)

The Al/Si in-depth profiles of three kinds of zeolites were analyzed by destructive and non-destructive XPS depth profiling methods. The destructive method with the use of $Ar^+$ sputtering resulted in serious distortion of the profiles due to preferential sputtering. As an alternative method, inelastic peak shape analysis was proposed to reveal the in-depth structure of non-planar surface materials. Peak energy referencing to the C*1s* line of the adventitious carbon was not a suitable method to discuss the chemical shift as small as 0.1-0.2 eV for zeolite that was a typical insulating and porous material. Instead, the use of "binding energy difference", such as Auger parameters, was recommended. For instance, formation of $Al_2O_3$ matrix was suggested on the external surface of steaming-dealuminated zeolite by the use of Al*2p-KLL* Auger parameter,

## 1. Introduction

XPS has long been applied to the surface and electronic structure analyses of zeolitic materials. The surface Al/Si ratios were discussed in comparison with the bulk ratios [1, 2]. The Auger parameters of various aluminosilicate compounds were investigated to analyze the local environment around Al and Si [3]. More recently, the O*1s* binding energy was discussed in relation to the charge density on oxygen that directly affects the acid strength of zeolite [4]. These past studies dealt with "extreme zeolite samples" in order to correlate the XPS information to zeolite properties. For instance, the chemical shifts of photoelectrons were often compared among the faujasite zeolites with very different Al/Si ratios, from NaA (Al/Si=1.0) to NaY (Al/Si~2.5).

Another interest of XPS analysis can be found in the detection of small changes of the zeolite characteristics that sometimes lead to critical improvements of the performance in the practical application. However, one cannot avoid some inherent problems of XPS analysis of zeolite, insulating and porous powders, that often hinder the application of sophisticated analytical methods. In the present study, we analyze practically important Na- and H-type faujasite zeolites with low Al/Si ratios (NaY and HY). The focuses of the analysis are on the Al/Si in-depth profiles and chemical state identification of Al using Al*2p* and Al*KLL* lines. Along with the discussions on these subjects, we discuss the above-mentioned problems in the XPS analysis of zeolites.

## 2. Experimental

All the spectra presented in this paper were measured on a PHI-5400 spherical capacitor analyzer with Mg Kα (1253.6 eV, 300 W) excitation. The Al*KLL* and Si*KLL* lines were excited with bremsstrahlung from the Mg anode. The energy scale of the spectrometer was calibrated using Au*4f5/2* (84.00 eV) and Cu*2p3/2* (932.40 eV) peaks. All the peak energies were corrected using the C*1s* line of the adventitious carbon at 285.00 eV. For quantitative analysis of the atomic Al/Si ratios, photo-ionization cross section table by Yeh and Lindau [5] was used. The pressure of the analysis chamber was below $2x10^{-9}$ torr during the measurements. Sputtering depth profiling was performed using a 2-keV $Ar^+$ beam with a current density of 3.4 $nA/mm^2$. Sputtering rate of zeolite under these conditions was estimated at about 1.6 nm/min.

The zeolite samples used in the present study were NaY zeolite powders (about 0.3 μm in diamater, YZ1, $Na_2O$=7.09%, Al/Si= 0.34) supplied by the Toso Corporation and their derivatives. Ion-exchanged HY zeolite (YZ2, $Na_2O$=0.68%, Al/Si=0.31) was prepared by double ion exchange of YZ1 using an aqueous $(NH_4)_2SO_4$ solution, followed by drying and calcination at 600 °C and steaming-dealuminated zeolite (YZ3, $Na_2O$=0.31%,

Al/Si=0.31) was obtained by another ion exchange of YZ2 followed by water vapor treatment for 1 h at 650 °C. Physical mixtures of $\gamma$-$Al_2O_3$ and $SiO_2$ powders with different Al/Si ratios (PM) were prepared as references. Prior to the measurements, all the powder samples were pressed into thin disks with a diameter of 10 mm.

### 3. Results and discussion

3.1 In-depth Al/Si profile

Fig. 1 shows the changes in Al/Si, Na/Si and C/Al ratios of YZ1 with $Ar^+$ sputtering. With increasing sputtering time, the Na/Si and C/Al ratios sharply decreased, while the Al/Si ratio was almost at constant. This is inconsistent with the nature of NaY zeolite in which Na is located adjacent to Al to compensate for the negative charge. Sputtering in association with surface charging presumably caused rapid migration of Na cations into the bulk. It is also inferred that the ion-exchangeable Na ions were preferentially sputtered compared with the matrix species, Al and Si. The XPS determination gave a surface Al/Si ratio of 0.36 that was similar to the value by chemical analysis (0.34). This suggests an almost even distribution of Al/Si ratio from the surface to the bulk. In past studies, XPS analysis generally gave Al/Si ratios consistent with chemical analysis, probably because some experimental errors were cancelled due to similar electron kinetic energies of Al2*p* and Si2*p*.

Fig. 2 shows the changes in the Al/Si ratios of YZ2, YZ3 and PM with $Ar^+$ sputtering. The Al/Si ratio of YZ2 monotonously increased with sputtering and was far beyond the bulk ratio of 0.31 after long sputtering. The Al/Si ratio of YZ3 at first decreased but began to increase after 15 min of sputtering. The minimum Al/Si ratio observed at 15 min of sputtering was significantly larger than that of the bulk. The profiles in Fig. 2 evidently indicate that the surface of YZ2 was rich in Si while that of YZ3 was rich in Al, as compared with the bulk. However, the profiles were significantly distorted by the preferential sputtering of Si compared with Al. Fig. 1 shows a constant Al/Si of YZ1 independent of sputtering time. During longer periods of sputtering, however, a similar increase of Al/Si was observed (not shown here). It is worth noting that the preferential sputtering could not be suppressed by decreasing the $Ar^+$ acceleration voltage down to 1 keV. In contrast to zeolite, the Al/Si profile of PM gradually decreased and was approaching to the bulk ratio of 0.48 with sputtering. Hence, the preferential sputtering of Si was found to be a characteristic phenomenon for zeolite matrix.

To eliminate the above problem associated with sputtering, non-destructive depth profiling was performed using inelastic peak shape analysis. Since the binding energies of Al2*p*, Si2*p*, Al2*s* and Si2*s* are too close, we analyzed Al*KLL* at −127 eV and Si*KLL* at −350 eV in the binding energy scale. Fig. 3 shows the comparison of Al*KLL* spectra of YZ1, YZ2

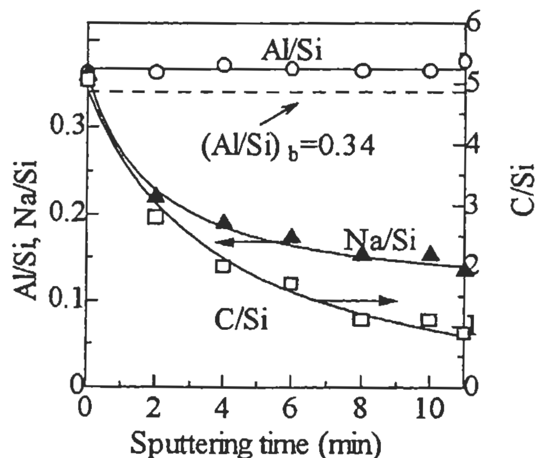


Fig. 1. Changes in Al/Si, Na/Si, and C/Si ratios of YZ1 with Ar ion sputtering

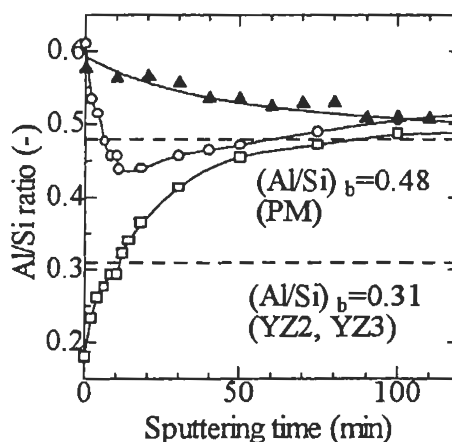


Fig. 2. Changes in Al/Si ratios with Ar ion sputtering ▫ YZ2 ∘ YZ3 ▲ PM

and YZ3. The intensity of the inelastic peak decreased in the order of YZ2 > YZ1 > YZ3. Considering the fact that photoelectrons from the bulk were subject to more energy loss events, surface enrichment of Al was in the order of YZ3 > YZ1 > YZ2. This is well confirmed by the comparison of Si*KLL* spectra shown in Fig. 4, which shows the decrease of the inelastic peak intensity in the order of YZ3 > YZ1 > YZ2.

The quantitative Al/Si profile could be deduced by the use of a software package "QUASES™" [6]. Al*KLL* spectra were more sensitive to the change of Al/Si profiles than Si*KLL*, because $SiO_2$ was the major component of zeolite. Hence, the Al*KLL* spectra of YZ2 and YZ3 were analyzed using the spectrum of YZ1 as a reference spectrum of homogeneous solid. With assumptions of exponential profiles and given bulk ratios, the parameters shown in Table 1 were obtained for YZ2 and YZ3.

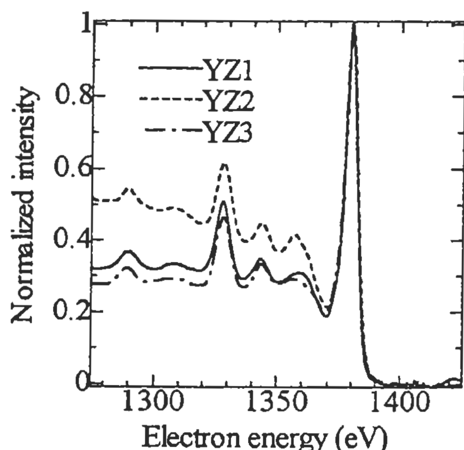

Fig. 3. Al KLL Auger specra of zeolite

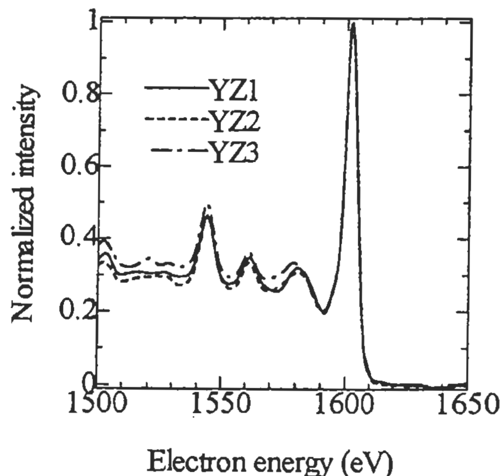

Fig.4. Si KLL Auger spectra of zeolite

Table 1 "QUASES" analysis of Al*KLL* spectra

| | (Al/Si) at surface | (Al/Si) in the bulk | Decay length |
|---|---|---|---|
| YZ2 | 0.0 | 0.31 | 70 Å |
| YZ3 | 1.2 | 0.31 | 50-80 Å |

Although the Al/Si ratios at surface in Table 1 (0.0 for YZ2 and 1.2 for YZ3) were not very likely, semi-quantitative profiles could be deduced by this method. At this stage, the analysis of inelastic peak shape gave qualitative but undoubted information on the in-depth profile. The calculation on many structural models, for instance stepwise profiles is needed for more precise results.

3.2 Chemical state identification

XPS gives information on the chemical state of zeolite matrix species that is directly related to the chemical properties. However, the precise determination of photoelectron energies is quite difficult due to heavy and sometimes uneven charging of insulating powdered materials. The primary subject before discussing the chemical state of zeolite is how to precisely determine the photoelectron binding energies.

Fig. 5 shows Al*2p* binding energies of zeolites and PM as a function of Si*2p* binding energy. For PM, the binding energies of Al*2p* were scattered with a standard deviation of 0.267 eV. A very good relationship between the binding energies of Al*2p* and Si*2p* suggests that the above scattering was caused by the fluctuation of C*1s* binding energies. Fig. 6 displays the C*1s* spectra of two PM samples that gave the largest difference in the Si*2p* binding energies. It is evidently shown that when the binding energies are referred to C*1s*, the peak determination within ±0.05 eV is not appropriate. In contrast, the standard deviation of Al*2p* lines was 0.077 eV when the binding energies were determined by referencing to the Si*2p* line. The plots of three zeolites in Fig. 5 indicate that the signals from Al in zeolite can be discriminated from those from $Al_2O_3$ matrix using the Al*2p* binding energy. At the same time, however, Fig. 5 indicates that referencing to the C*1s* line may result in an ambiguous discussion.

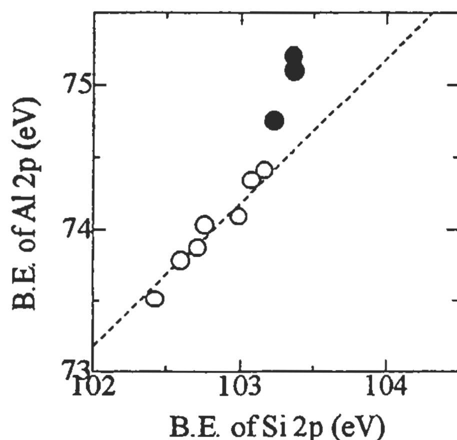


Fig.5. Binding energies of Al $2p$ as a function of Si $2p$
○ Phys. mix. of $Al_2O_3$ and $SiO_2$
● Zeolite (YZ1, YZ2, YZ3)

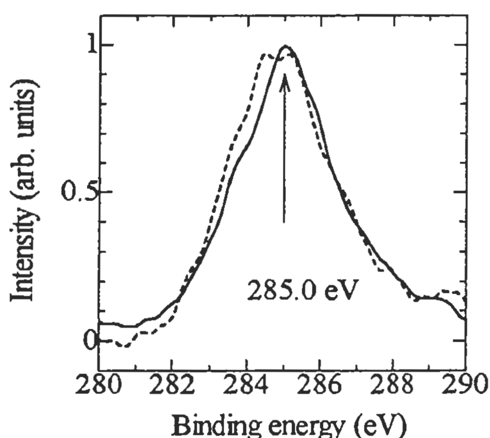


Fig. 6. C $1s$ spectra of two physical mixtures of $Al_2O_3$ and $SiO_2$

To minimize the above-mentioned ambiguity, we performed "Auger parameter ($AlKL_{23}L_{23}$ energy + Al$2p$ binding energy)" plots as shown in Fig. 7 that evidences very small fluctuation of the Auger parameters among the five $\gamma$-$Al_2O_3$ samples. When the Auger parameters of the three zeolite samples are compared, YZ3 gave a slightly higher value than the other zeolites. The higher Auger parameters of zeolites than $\gamma$-$Al_2O_3$ are due to large extra-atomic relaxation energies, because Al atoms in zeolites are surrounded by "-O-Si" bonding. Thus, the small relaxation energy of YZ3 suggests formation of $Al_2O_3$ matrixes associated with the deterioration of zeolite framework at the external surface.

Thus, the use of energy differences in two photoelectron or Auger lines enabled

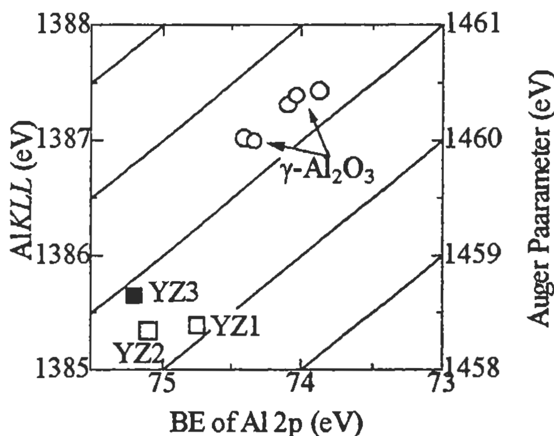


Fig. 7. Auger parameters obtained from Al$2p$ and Al$KLL$

meaningful discussions based on small chemical shifts. It should be noted that accurate methods for peak energy determination and energy scale calibration are essential for the maximal utilization of the energy differences.

## 4. Conclusion

The present study discussed two important subjects in the analysis of zeolitic materials, insulating and porous powders. As regard to the analysis of in-depth profiles, the use of sputtering depth profiling was found to give distorted profiles due to surface charging and preferential sputtering. Rather, the use of inelastic peak shape analysis was recommended.

For chemical state identification, the peak energy referencing to the C$1s$ line may result in large errors. The use of "binding energy difference" was found to enable the discussion based on chemical shifts as small as 0.1-0.2 eV.

## References

[1] E. G. Derouane, J. P. Gilson, Z. Gabelica, C. M. Desbuquoit, J. Verbist, J. Catal., 71, 447 (1981).

[2] T. L. Barr and M. A. Lishka, J. Am. Chem. Soc., 108, 3178 (1986).

[3] C. D. Wagner, D. E, Passoja, H. F. Hillery, T. G. Kinisky, H. A. Six, W. T. Jansen J. A. Taylor, J. Vac. Sci. Technol., 21, 933 (1982).

[4] Y. Okamoto, M. Ogawa, A. Maezawa, T. Imanaka, J. Catal., 112, 427 (1988).

[5] J. J. Yeh and I. Lindau, Atomic and Nuclear Data Tables, 32 (1985) 155.

[6] S. Tougaard, Applied Surf. Sci., 100/101, 1 (1996).